

Offline Model Based MTPA Methodology for Optimum Performance of Interior Permanent Magnet Machines over Full Range of Speed and Torque

Visweshwar Chandrasekaran¹, Member, IEEE, Bernard Jose², Member, IEEE, Ashwin Karthik Muralidharan³, Member, IEEE
Ned Mohan^{*}, Life Fellow, IEEE, Kaushik Basu[§], Senior Member, IEEE

Email: viswesh@umn.edu, bernard.jose@tranetechnologies.com, ashwin.muralidharan@colorado.edu, mohan@umn.edu, kbasu@iisc.ac.in

¹Trane Technologies, St. Paul, MN, USA, ²Trane Technologies, Bangalore, India, ³BREK Electronics, Denver, CO, USA

^{*}Department of Electrical and Computer Engineering, University of Minnesota, Minneapolis, MN, USA

[§]Division of EECS, Indian Institute of Sciences, Bangalore, India

Abstract— There has been a growing adaptation of Variable Frequency Drives (VFD) for motor applications in all areas. Maximum Torque Per Ampere (MTPA) algorithms are common solutions that aim at achieving efficient operation of drives. This paper presents a novel offline MTPA trajectory generation scheme for an interior permanent magnet (IPM) motor drive. The proposed approach is based on calculating the minimum current possible for every load operating point by solving for polynomial roots of the torque expression in a closed form solution and considers non-linear saturation and cross-coupling properties of the IPM machine. The offline calculation and state logic have been implemented using a model-based design approach and key considerations have been made for efficient execution while minimizing computational resource requirements, thus expanding the deployment scope on a wide range of motor drives including cost sensitive applications. Experimental results obtained on a 3HP IPM motor demonstrate the effectiveness of the proposed scheme in achieving the MTPA control objective while maintaining control stability across all operating regions.

Keywords— maximum-torque-per-ampere (MTPA), interior permanent magnet machine (IPM), motor drive, variable frequency drive (VFD), inverter efficiency, field oriented control (FOC)

I. INTRODUCTION

Power Electronic equipment such as Variable Frequency Drives (VFDs) are seeing increased usage in motor applications. This is due to the increased efficiency achieved by VFDs and the ability to precisely control factors such as speed and torque for the entire operation map of the equipment. IPM machines have also gained significant popularity over the last several decades due to several advantages that include high power density and absence of rotor losses. However, the rotor construction in an IPM machine while taking advantage of dual torque mechanisms results in high magnetic saliency. This is reflected in non-equal quantities for the DQ axis inductances. Several research works take advantage of this phenomenon to extend and even optimize the machine design to operate under extended speed and torque range very efficiently [1][2].

A popular scheme for IPM machines is MTPA which aims to deliver maximum efficiency across wide range of operation. A

broad classification of various MTPA schemes is summarized in [3]. Initial research focused on maximizing efficiency for entire speed range [4][5]. It is most typical to formulate MTPA schemes based on predetermined tuning coefficients in combination with active and adaptive estimation and tracking [6][7]. Online MTPA schemes employ either minimum current search, signal injection or model-based techniques [8][9]. The performance of any MTPA scheme is dependent on accurate knowledge of motor parameters. The non-linear parameters of an IPM include (but not limited to) – stator resistance and magnet flux linkage (both of which vary with motor temperature) [10] and the d – and q – axis flux linkages (and hence inductances) which vary with d – and q – axis currents at a given operating point [11]. While online methods aim to achieve parameter insensitive execution, the implementation can be quite complex especially in cost sensitive applications and many methods still rely on Look Up Tables (LUTs) [12]. Several offline methods have been proposed which generate LUTs which may require large amount of memory and accurate interpolation algorithms [14].

To develop an offline calculation of MTPA, 2D LUTs of the d – and q – axis flux linkages are obtained via Finite Element Modelling of the IPM machine. For the given motor sample, a teardown analysis was performed to obtain key information of the stator and rotor geometries as seen in Fig. 1.

In this paper, a cost and memory optimized offline LUT based MTPA scheme is proposed with singular array data for the current magnitude corresponding to every operating load point. The overall search algorithm for determining minimum current for every operating Torque is discussed, and experimental study was carried out on a motor drive system to verify MTPA control along the proposed current trajectory.

II. CONVENTIONAL MTPA THEORY

The IPM machine is modelled in the synchronous DQ frame and is given by (1-2). Due to the saliency in the rotor as a result of magnet placement, the flux distribution between the D and Q axis are unique and are exhibited in the flux linkages λ_{ds} and

λ_{qs} . Furthermore, there exists a self and cross-coupling effect of the DQ axis currents on the flux linkages as given by (3-4).

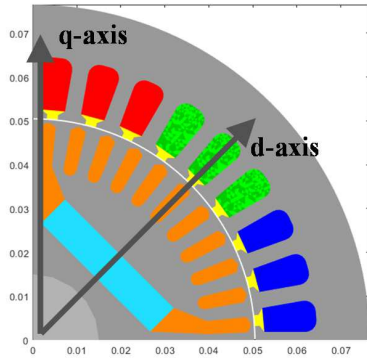


Fig. 1. Four Pole IPM geometry showing rotor magnet profile including rotor bars to aid in line-starting the machine

Fig. 2 describes the voltage and current relationships in the DQ frame. The current angle, γ is defined as the angle between the Q axis current, I_{qs} and the net space vector current, I_{qds} of the machine at any given operating point. The work in this paper proposes a novel scheme to identify the optimal current angle and the corresponding least possible space vector current for every load operating point of the given IPM machine. It is well established in literature [2][17] that IPM machines have both self and cross saturation effects which result in 2D flux linkage or inductance maps that can be obtained either experimentally or via Finite Element Analysis (FEA) having knowledge of the machine geometry. These maps are shown in Fig. 3.

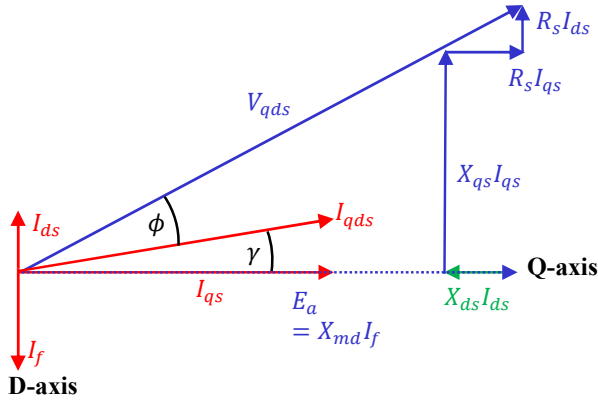


Fig. 2. Vector diagram of IPM voltage and current relationships

$$V_{qs} = R_s I_{qs} + \frac{d\lambda_{qs}}{dt} + \omega_e \lambda_{ds} \quad (1)$$

$$V_{ds} = R_s I_{ds} + \frac{d\lambda_{ds}}{dt} - \omega_e \lambda_{qs} \quad (2)$$

Where,

$$\lambda_d = L_{dd}(I_{ds}, I_{qs})I_{ds} + L_{dq}(I_{ds}, I_{qs})I_{qs} \quad (3)$$

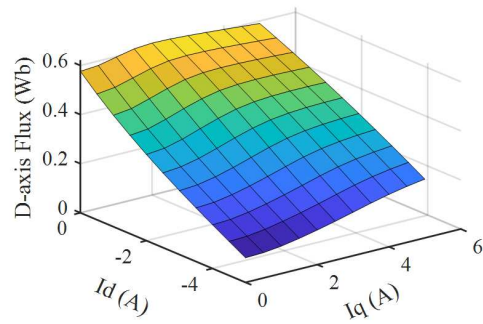
$$\lambda_q = L_{qd}(I_{ds}, I_{qs})I_{ds} + L_{qq}(I_{ds}, I_{qs})I_{qs} \quad (4)$$

For an IPM machine the d – and q – axis inductances are not equal to each other which results in two torque mechanisms – magnet flux and reluctance torque given by (5) and further expressed in terms of DQ flux and currents as seen in (6)

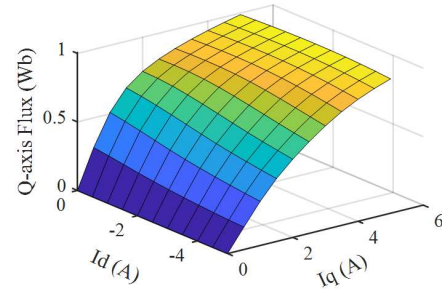
$$T_{em} = T_{mag} + T_{rel} \quad (5)$$

$$T_{em} = \frac{3P}{2} (\lambda_d I_{qs} - \lambda_q I_{ds}) \quad (6)$$

In the conventional MTPA formulation, a simplifying assumption is often made to fix a single value of DQ inductance to derive the torque and current angle expressions. For a fixed value of inductance and ignoring machine saturation, (1) and (2) can be simplified to (7) and (8) respectively while (6) can be expanded in terms of DQ currents and Inductances as seen in (9).



(a)



(b)

Fig. 3. 2D flux maps for (a) d-axis and (b) q-axis generated via FEA simulations

$$V_{qs} = R_s I_{qs} + L_q \frac{dI_{qs}}{dt} + \omega_e L_d I_{ds} + \omega_e \lambda_{pm} \quad (7)$$

$$V_{ds} = R_s I_{ds} + L_d \frac{dI_{ds}}{dt} - \omega_e L_q I_{qs} \quad (8)$$

$$T_{em} = \frac{3P}{2} [\lambda_m I_{qs} + (L_d - L_q) I_{qs} I_{ds}] \quad (9)$$

From (8) it can be observed that when I_{ds} is fixed to a constant value (often simplified to $I_{ds} = 0$ for low-performance drives), the electromagnetic torque can be easily controlled by manipulating the I_{qs} quantity [17]. However,

this simplification does not fully utilize the reluctance principle present in the IPM machine which is best utilized when I_{ds} is a dynamic non-zero quantity, changing with the operating point. This will result in a complex solution for determining the best combination of (I_{ds}, I_{qs}) to achieve the desired torque at the operating condition. The maximum output torque of an IPM is decided by the current and voltage limits which are represented by (10) and (11). The current limit circle is visualized in Fig. 5 for the motor being studied in this paper.

$$\sqrt{I_{ds}^2 + I_{qs}^2} \leq I_{qds} \quad (10)$$

$$\sqrt{V_{ds}^2 + V_{qs}^2} \leq V_{qds} \quad (11)$$

For a given torque demand at an operating point, line current amplitude is minimized to achieve the maximum torque. By placing the constraint of (9), the expression in (8) can be rewritten to express torque as a function of I_{ds} and is given by (12)

$$T_{em} = \frac{3P}{2} \left[\lambda_m * \sqrt{(I_{qds})^2 - (I_{ds})^2} + I_{ds}(L_d - L_q) \sqrt{(I_{qds})^2 - (I_{ds})^2} \right] \quad (12)$$

Now, for the MTPA objective, a derivative of the above expression w.r.t I_{ds} can be written and solved (as in $\frac{dT_{em}}{dI_{ds}} = 0$) to find the minimum solution of current to achieve demanded torque. This gives an expression for I_{qds} given by (13)

$$I_{qds} = \sqrt{2I_{ds}^2 + \frac{\lambda_m I_{ds}}{(L_d - L_q)}} \quad (13)$$

This expression for I_{qds} can then be substituted into (12) and simplified to yield the below expression for torque as a function of d-axis current only as given by (14)

$$T_{em} = \frac{3P}{2} \left[\sqrt{I_{ds}^2 + \frac{\lambda_m I_{ds}}{(L_d - L_q)}} \right] \left[\lambda_m + (L_d - L_q) I_{ds} \right] \quad (14)$$

Using (14) and (9) a closed form solution can be obtained for $T_{em}(I_{ds}, I_{qs})$ for every operating point which satisfies the MTPA objective. For a simple model of the IPM machine ignoring flux/inductance saturation and keeping magnet flux linkage as constant, the MTPA trajectory follows the conventional line shown in Fig. 5.

An alternate solution for determining the optimal current angle for every operating point is well reported in literature [19][7][20] and is given by (15)

$$\gamma = \sin^{-1} \left(\frac{-\lambda_m + \sqrt{\lambda_m^2 + 8(L_d - L_q)I_{qds}^2}}{4(L_d - L_q)I_{qds}} \right) \quad (15)$$

As mentioned previously, in considering the above analytical approaches to solve for MTPA condition, motor parameters such as L_d, L_q and λ_m are considered constant and independent of motor operating point. This implies that the effects of self- and cross-saturation are being ignored. The goal of this study is to examine and formulate an offline MTPA trajectory while considering the non-linear properties of the IPM machine such as flux saturation with load. The non-linear property of PM flux linkage and hence back electro-motive force (BEMF) variation as a function of temperature is kept out of the scope of this paper as all experiments were conducted while keeping the motor sample at room temperature. Further reading on this subject can be found in [17] and [18].

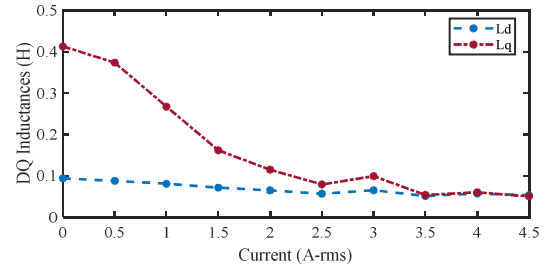


Fig. 4. Profile of d- and q-axis inductances showing non-linear saturation

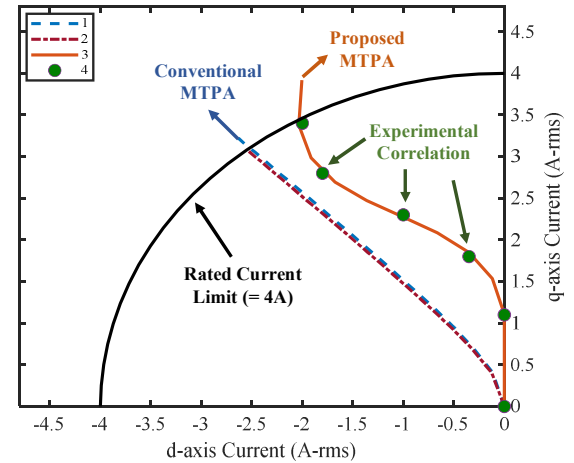


Fig. 5. MTPA trajectories showing results for conventional methods in 1—fixed inductances from vendor datasheet, 2—fixed unsaturated inductance from FEA, 3—proposed method considering inductance saturation and 4—experimental testpoints matching proposed trajectory

III. MTPA TRACKING FORMULATION CONSIDERING MACHINE SATURATION

A suitable method for obtaining MTPA for an IPM machine considers a closed form solution for minimum current for demanded torque at every operating point while considering the non-linear properties of the machine's parameters – namely L_d and L_q . Looking at Fig. 2, the DQ axis currents can be represented in terms of the net space vector current as,

$$I_{qs} = I_{qds} \cos(\gamma) \quad (16)$$

$$I_{ds} = -I_{qds} \sin(\gamma) \quad (17)$$

The resultant electromagnetic torque expression for the IPM machine can be expanded from (3) making use of (6) and (7) to result in

$$T_{em} = \frac{3P}{4} (\lambda_{PM} I_{qds} \cos(\gamma) - (L_{ds} - L_{qs}) I_{qds}^2 \cos(\gamma) \sin(\gamma)) \quad (18)$$

Considering the saturation properties of the machine the inductances for every operating point are obtained from the FEA generated 2D flux maps such that the saturated inductance – i.e., $L_d(I_{ds}, I_{qs})$ and $L_q(I_{ds}, I_{qs})$ shall be used to solve for torque in (18). The above expression can further be expressed in terms of a polynomial w.r.t to the d -axis current as given by (19). The solution can be derived by solving for the positive real roots of the expression as given by (20)

$$K_a I_{qds}^2 + K_b I_{qds} + K_c = 0 \quad (19)$$

$$I_{qds} = \text{real} \left[\frac{-K_b \pm \sqrt{(K_b^2 - 4K_a K_c)}}{2K_a} \right] \quad (20)$$

while the coefficients in (19) are given by,

$$K_a = -\frac{3P}{4} (L_{ds} - L_{qs}) \cos(\gamma) \sin(\gamma);$$

$$K_b = \frac{3P}{4} \lambda_{PM} \cos(\gamma) \text{ and}$$

$$K_c = -T_{em}.$$

IV. PROPOSED MODEL BASED OFFLINE MTPA SCHEME

The MTPA tracking technique proposed in this paper is based on identifying the minima of the roots of the polynomial that solves for the space vector current, I_{qds} for every operating load condition. To achieve a simple yet robust approach to solving for the MTPA trajectories, a novel model based iterative design is introduced in this work. Having knowledge of the rated load torque of the machine and fixing a range of current angles $[0: \gamma_{max}]$, it is possible to scan through each operating condition of torque and solve for all values of γ and I_{qds} . Motor nameplate parameters are inputs to the MTPA scheme and resulting outputs are Look Up Table (LUT) arrays of space vector current, $I_{qds(MTPA)}$ and current angle γ_{MTPA} . A flowchart of the proposed scheme is shown in Fig. 6 showing a nested loop structure. To further elaborate, the electromagnetic torque, T_{em} is fixed at a certain value and the current angle is scanned through the pre-designated range. For the various current angles, the combination of (L_d, L_q) is selected from the 2D FEA LUTs. All real positive solution for the roots of (19) are solved as shown in (20). Then the minimum solution is picked using a Sample and Hold logic. By this logic, the proposed scheme can also be stated as Minimum Current Per Torque (MCPT) considering the inverted logic of finding minimum current for every operating point.

At the next iteration, the torque reference is incremented by a certain factor and a new minimum result is computed using the same procedure outlined considering a selection of L_d, L_q and γ as the changing variables for the quadratic expression. The resultant optimal values of space vector current, I_{qds} and current angle, γ are stored into 1D LUTs. The generated arrays can then be utilized in a FOC scheme for the IPM machine. The results for MTPA currents and current angle for zero to rated torque conditions for the 3HP IPM machine used in this study are shown in Fig. 11(a) and (b).

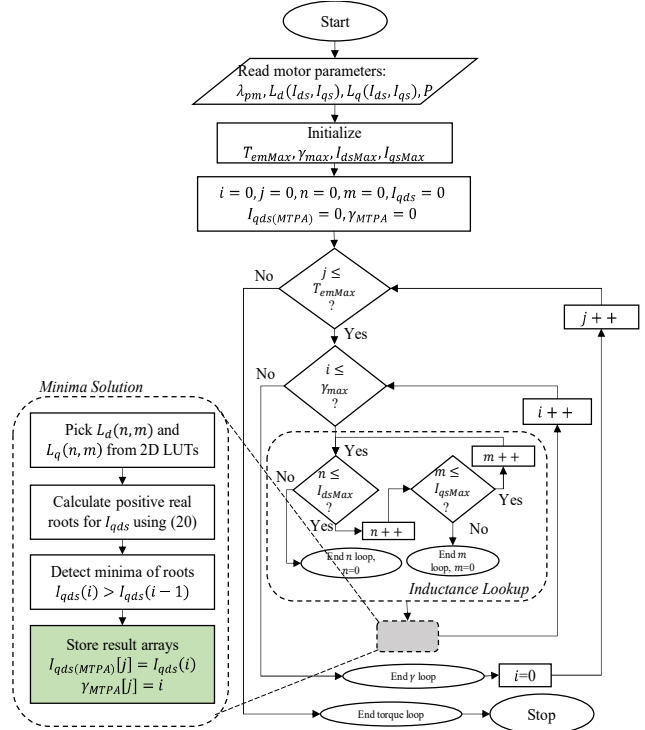


Fig. 6. Proposed flowchart for generating the MTPA LUT data for current and gamma angles for all load operating conditions

A model-based approach is taken in implementing the described offline trajectory generation scheme and is graphically represented in Fig. 7. Several considerations have been made to reduce arithmetical and logical complexity and a summary of design elements is shown in Table I. This enables the scheme to be implemented in medium to low performance microcontrollers and unlocks the potential for wider application of the MTPA logic in cost sensitive motor drive applications.

TABLE I. DESIGN ELEMENTS IN MODEL BASED MTPA GENERATION SCHEME

Element	Count
Add/Subtract	10
Multiply	18
Divide	4
Trigonometric	2
Relational	5
Square Root	1

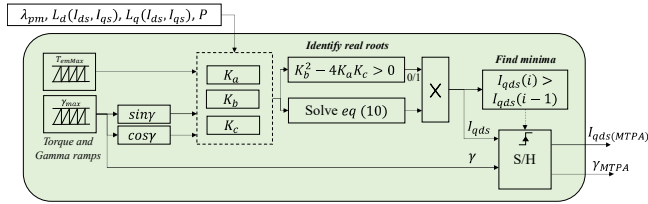


Fig. 7. Model Based design of the offline MTPA trajectory generation scheme

The proposed offline MTPA scheme is quite dependent on the machine parameters for the calculation of the coefficients and to solve for the real positive roots for minimum current detection. Having good knowledge of the parameters is paramount to the accuracy of the proposed scheme.

As a case study, Fig. 8 captures the multiple solutions of current, I_{qds} , to achieve the demand torque. This data is solved for the various combinations of $L_d(I_{ds}, I_{qs})$ and $L_q(I_{ds}, I_{qs})$ sourced from FEA data shown in Fig. 3. The optimal solution lies along the trajectory highlighted in dashed red while the other operating points may still generate torque albeit at a poorer control efficiency.

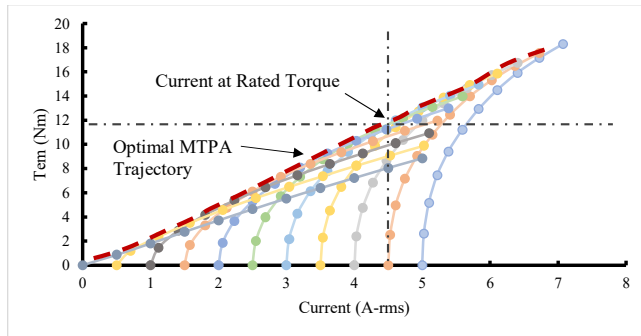


Fig. 8. Graph showing multiple solutions for stator currents for every operating point and MTPA trajectory optimizing current for each torque

The result of employing the proposed offline MTPA algorithm is shown in Fig. 10 and 11 and in Fig. 5. Three methods to obtain MTPA solution are analyzed and compared –

- M1. Conventional method using motor supplier provided datasheet
- M2. Conventional method using unsaturated DQ inductances obtained from FEA analysis
- M3. Proposed MTPA method using saturation inductances from FEA analysis

The methods M1 and M2 show close correlation in the solution for current angle, γ and MTPA current for all operation points. However, there is significant deviation from the results of method M3 which utilizes the saturation profile

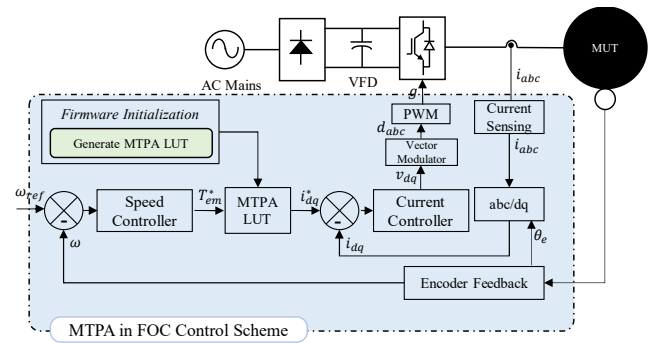


Fig. 9. Overall block diagram of the proposed MTPA algorithm used in a FOC motor control scheme

of the DQ inductances to solve for MTPA trajectories. Current magnitudes for different angles are shown in Fig. 10.

Following the description of the proposed MTPA algorithm, for a fixed torque, T_{em} , a sweep of current angles from $0 - 80^\circ$ is performed. An optimal angle results in the minimum current to deliver the required torque. With the idealized parameters of M1 and M2, the angle trajectory follows an exponential trend which saturates closer to 40° . However, when using saturation profiles, one can observe that the current angle remains at 0° until 1 A-rms of space vector current after which the angle grows. This indicates that the low torque conditions can be delivered without any d -axis current injection. Another observation that can be made is that with M3 trajectory, there is an overall lesser magnitude of current angle even at full rated condition, as seen in Fig. 11(a), indicating less requirement to de-flux the machine at full load. Further to this, Fig. 11(b) indicates a slightly reduced requirement of current magnitude for M3 when compared to M1 and M2 which concludes that by accounting for machine saturation properties in MTPA calculations, a better utilization of current is possible to achieve the same levels of torque when compared to the conventional MTPA methods.

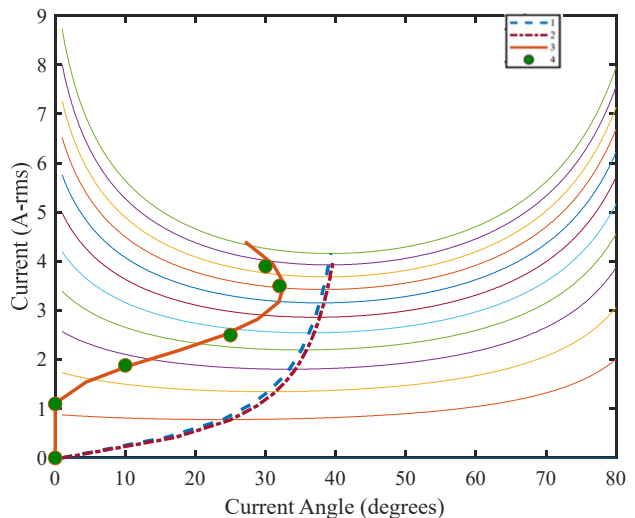


Fig. 10. Implementation of proposed model based search algorithm identifying minimum current solution and corresponding current angle for each iteration of torque are shown for the conventional methods M1 and M2 as well as proposed method M3 along with experimental test data.

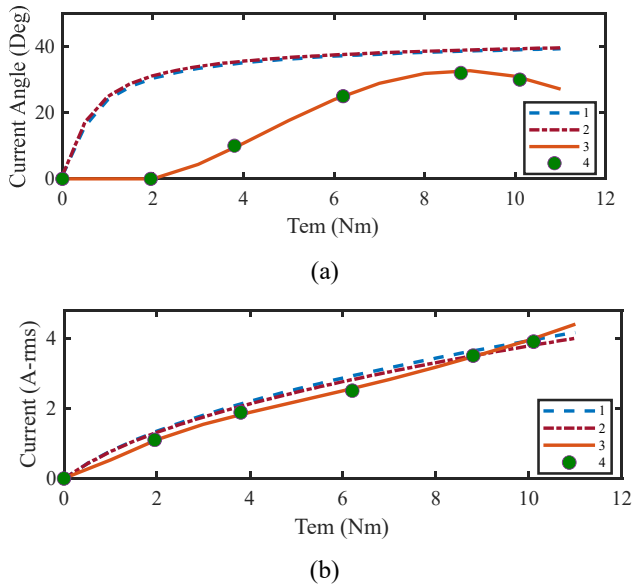


Fig. 11. Current angle (a) and RMS current (b) relationship with torque for zero rated condition are shown for all three methods M1-M3 along with test datapoints

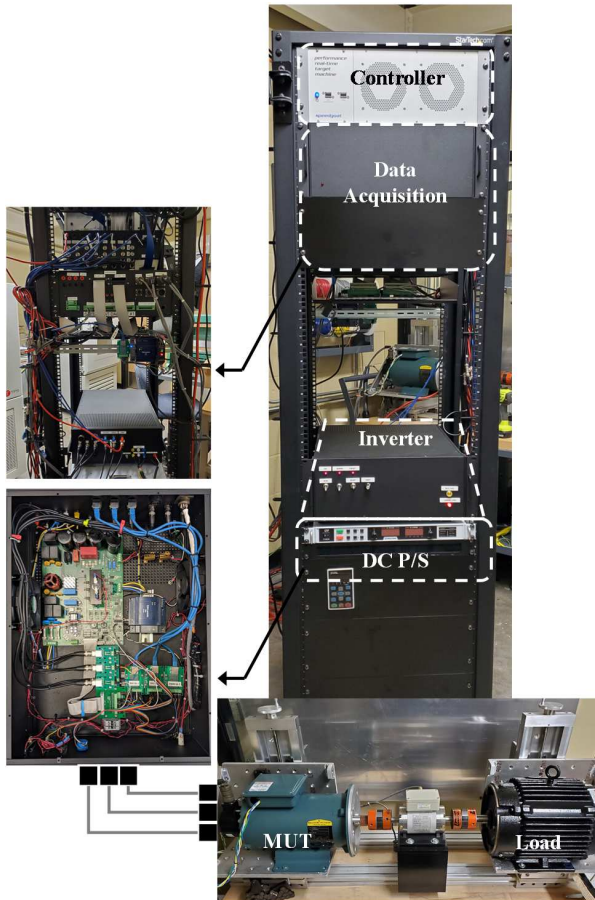


Fig. 12. Experimental setup of a 3HP IPM Motor-Under-Test (MUT) coupled to a matched 3HP PM based load motor. MUT driven via classic 2-L VSI DC-fed Inverter

V. EXPERIMENTAL VALIDATION

In this section, experimental results are presented to demonstrate the accuracy of the MTPA trajectory obtained via the proposed model based offline scheme. A state machine first starts the controller into “initialization” state which enables the offline MTPA trajectory calculation and the resulting LUT arrays for space vector current, $I_{qds(MTPA)}$ and current angle γ_{MTPA} are stored in memory. The state machine then goes to “active” state which starts the motor control scheme. The MTPA LUTs are utilized to generate the corresponding DQ current references for the inner current/torque regulator while taking the reference electromagnetic torque signal calculated by the outer speed regulator. The proposed model based MTPA scheme as well as the FOC control algorithm has been developed in MATLAB/Simulink and auto-code generation tools have been used to generate the code. The code has been deployed on a Performance Real-Time target from Speedgoat. The Speedgoat controller consists of a 4.2 GHz Quad core Intel i7 CPU operating with Simulink Real Time operating system. The peripherals such as Analog, Digital I/O’s as well as PWM are implemented on a Xilinx Kintex-7 FPGA option card called IO334 with a based clock rate of $10ns$. While this controller significantly exceeds the requirements of the proposed control scheme, the authors have taken advantage of the rapid prototyping capabilities offered by Speedgoat.

A power inverter has been developed based on the classic 2-Level (2L) Voltage Source Inverter (VSI) topology. An evaluation board with P/N: EVAL-M5-IMZ120R-SIC has been sourced from Infineon Technologies for the power inverter. A custom data acquisition system has also been developed to measure various feedback quantities such as quadrature encoder, shaft torque, motor voltages and currents. The MUT used in this study is a 3HP IPM from Baldor with P/N: CSPM3611T while the load motor is a 3 HP IPM from Marathon with P/N SY006A. The vendor provided datasheet is shown in Table II. The load motor is connected to a resistive load bank via a three-phase autotransformer to adjust the shaft load for each operating speed.

TABLE II. IPM Motor Parameters from Vendor Datasheet

Parameter	Value
Rated Power	3 HP
Rated Voltage	460 V – rms
Rated Speed	1800 r/min
Rated Current	4 A – rms
Rated Torque	12 Nm
Stator Resistance, R_s	2.184 Ω
Direct Axis Inductance, L_d	10.393 mH
Quadrature Axis Inductance, L_q	300 mH
Magnet Flux Linkage, λ_{pm}	0.376 Wb
No. of Poles, P	4
Inertia, J	0.011 kg.m ²

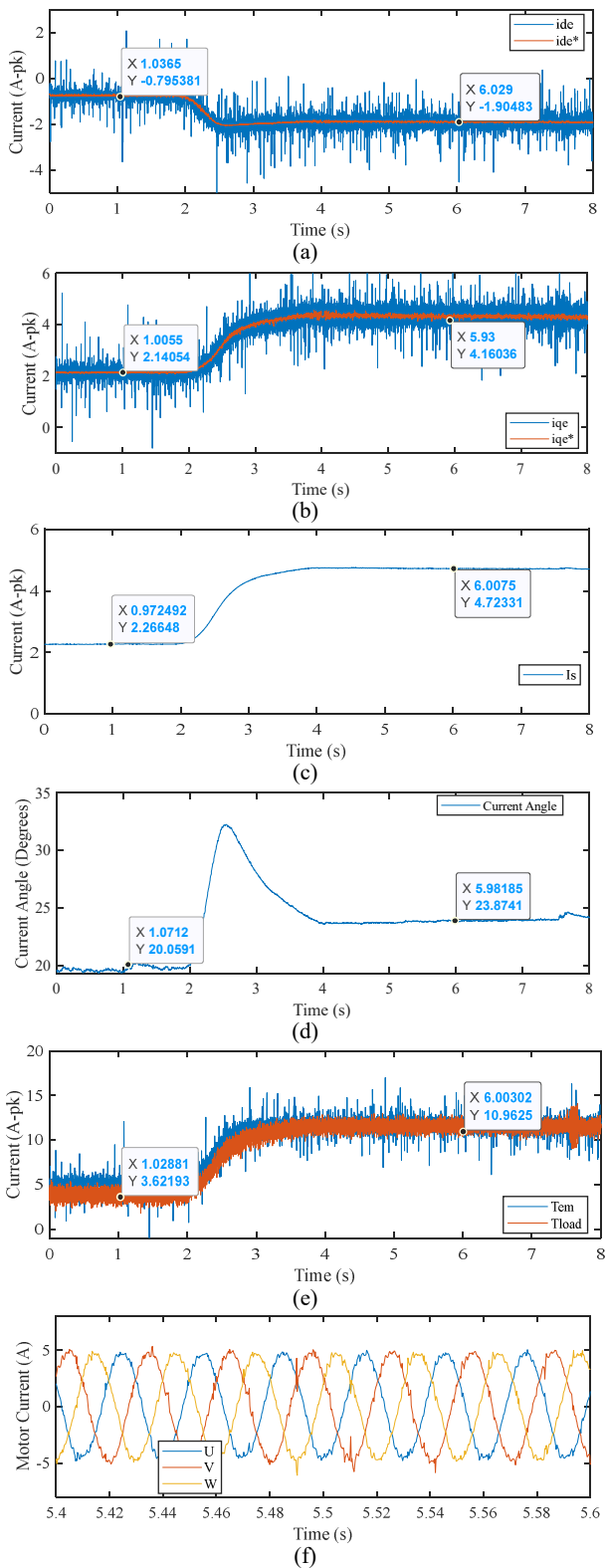


Fig. 13. Experimental results showing D-axis and Q-axis current tracking in (a) and (b), Current Space Vector in (c), Current Angle calculated via proposed MTPA algorithm in (d), Electromagnetic Torque estimated via controller and load torque measured in (e) and 3 phase motor currents zoomed into a steady state region in (f)

The control scheme is implemented with the outer speed regulator running at 5Hz bandwidth while the inner current regulator is running at 100Hz. The inverter switching frequency is programmed at 4kHz which represents a typical configuration for most industrial drives across multiple industries. The details of the controller design are beyond the scope of this paper and can be found in [15]. Task execution time (TET) is defined as the time taken by the kernel to run for one base-rate time step while real time budget (RTB) is defined as the % of TET over the time step period given in (21). The average TET for the FOC control was measured to be 87.5 μ s which yields an RTB of 35%. A good design principle is to maintain RTB <50% to allow for robust operation and code expansion and it can be seen that the FOC control including MTPA scheme achieves the RTB target.

$$RTB = \frac{Bus\ Clock\ Ticks}{Control\ Time\ Step} * 100\ \% \quad (21)$$

Fig. 13 show the experiment results for two steady state operating points to determine the quantities such as I_{ds} , I_{qs} , γ , and T_{em} and compare them against the theoretical MTPA trajectory. The MUT is operated at 1000 r/min with an initial load of ~40% and at $t = 2s$ the load is manually adjusted to ~83.5%. Fig 13(a) and (b) show stable tracking of the DQ currents by the current regulators while (d) shows the current angle, γ , at these operating points; (e) shows calculated electromagnetic torque as well as measured load torque and finally (f) shows the three phase motor currents. It is to be noted that there will be practical differences between the electromagnetic torque and mechanical output load torque owing to core losses in motor as well as mechanical losses in the shaft assembly. Characterizing these losses is beyond the scope of this paper and is detailed in [16]. Steady state points obtained via experiments are overlaid onto the proposed trajectory in Fig. 5, 10 and 11 which show the tracking error of the algorithm to be under 1%. This confirms that the offline calculated LUTs for $I_{qds}(MTPA)$ and γ_{MTPA} match the real motor operating conditions with good accuracy.

VI. CONCLUSIONS

The torque production of an IPM machine over its operating speed range has strong dependency on the allocation of net current between the d – and q – axis components. The MTPA condition is affected by the machine's parameters along with flux saturation plays a significant role. The work in this study proposes an offline LUT generation scheme which considers inductance variation across operating map and calculates the optimal current angle, γ which helps achieve minimum current for the torque demand. This method works consistently across the speed range of the machine as the mechanical time constant doesn't impact the torque optimization objective. State of the art model based design and code generation techniques have been adapted which accelerates the design and validation stages. The offline algorithm is constructed with a focus on minimizing the computational demand thus enabling wider adaptation in cost sensitive applications. Simulation and experimental results show tight correlation with less than 1% error in optimized current for the given torque demand.

The proposed method does not require additional hardware or controller capabilities beyond standard motor drive technology. This provides a big advantage in realizing the solution across multiple applications and industries such as automotive, aerospace and industrial automation.

REFERENCES

- [1] Morimoto, Shigeo, et al. "Expansion of operating limits for permanent magnet motor by current vector control considering inverter capacity." *IEEE transactions on industry applications* 26.5 (1990): 866-871.
- [2] Bianchi, Nicola, and Thomas M. Jahns. "Design analysis and control of interior PM synchronous machines." *Tutorial Course Notes, IEEE-IAS 4* (2004).
- [3] Tinazzi, F., et al. "Classification and review of MTPA algorithms for synchronous reluctance and interior permanent magnet motor drives." *2019 21st European Conference on Power Electronics and Applications (EPE'19 ECCE Europe)*. IEEE, 2019.
- [4] R. F. Schiferl and T. A. Lipo, "Power capability of salient pole permanent magnet synchronous motors in variable speed drive applications," *IEEE Trans. Ind. Appl.*, vol. 26, no. 1, pp. 115–123, Jan 1990
- [5] S. Morimoto, M. Sanada, and Y. Takeda, "Wide-speed operation of interior permanent magnet synchronous motors with high-performance current regulator," *IEEE Trans. Ind. Appl.*, vol. 30, no. 4, pp. 920–926, July 1994
- [6] Dianov, Anton, et al. "Robust self-tuning MTPA algorithm for IPMSM drives." *2008 34th Annual Conference of IEEE Industrial Electronics*. IEEE, 2008.
- [7] Niazi, Peyman, Hamid A. Toliyat, and Abbas Goodarzi. "Robust maximum torque per ampere (MTPA) control of PM-assisted SynRM for traction applications." *IEEE transactions on vehicular technology* 56.4 (2007): 1538-1545.
- [8] Windisch, Thomas, and Wilfried Hofmann. "A novel approach to MTPA tracking control of AC drives in vehicle propulsion systems." *IEEE Transactions on Vehicular Technology* 67.10 (2018): 9294-9302.
- [9] Bolognani, S., L. Sgarbossa, and M. Zordan. "Self-tuning of MTPA current vector generation scheme in IPM synchronous motor drives." *2007 European Conference on Power Electronics and Applications*. IEEE, 2007.
- [10] S. Bolognani, R. Petrella, A. Prearo, and L. Sgarbossa, "Automatic tracking of MTPA trajectory in IPM motor drives based on ac current injection," *IEEE Trans. Ind. Appl.*, vol. 47, no. 1, pp. 105–114, Jan. 2011.
- [11] Sebastian, Tomy. "Temperature effects on torque production and efficiency of PM motors using NdFeB magnets." *IEEE Transactions on Industry Applications* 31.2 (1995): 353-357.
- [12] Sneyers, Brigitte, Donald W. Novotny, and Thomas A. Lipo. "Field weakening in buried permanent magnet ac motor drives." *IEEE Transactions on Industry Applications* 2 (1985): 398-407.
- [13] Kim, Sungmin, et al. "Maximum torque per ampere (MTPA) control of an IPM machine based on signal injection considering inductance saturation." *IEEE Transactions on Power Electronics* 28.1 (2012): 488-497.
- [14] Bae, Bon-Ho, et al. "New field weakening technique for high saliency interior permanent magnet motor." *38th IAS Annual Meeting on Conference Record of the Industry Applications Conference, 2003.. Vol. 2*. IEEE, 2003.
- [15] Chandrasekaran, Visweshwar, et al. "A novel model based development of a motor emulator for rapid testing of electric drives." *2020 IEEE Energy Conversion Congress and Exposition (ECCE)*. IEEE, 2020.
- [16] Xia, Zekun, et al. "Online optimal tracking method for interior permanent magnet machines with improved MTPA and MTPV in whole speed and torque ranges." *IEEE Transactions on Power Electronics* 35.9 (2020): 9753-9769.
- [17] Pellegrino, Gianmario, et al. *The rediscovery of synchronous reluctance and ferrite permanent magnet motors: tutorial course notes*. Springer, 2016.
- [18] Krishnan, R., and Praveen Vijayraghavan. "Fast estimation and compensation of rotor flux linkage in permanent magnet synchronous machines." *ISIE'99. Proceedings of the IEEE International Symposium on Industrial Electronics (Cat. No. 99TH8465)*. Vol. 2. IEEE, 1999.
- [19] Morimoto, Shigeo, et al. "Expansion of operating limits for permanent magnet motor by current vector control considering inverter capacity." *IEEE transactions on industry applications* 26.5 (1990): 866-871.
- [20] Morimoto, Shigeo, et al. "Servo drive system and control characteristics of salient pole permanent magnet synchronous motor." *IEEE Transactions on Industry Applications* 29.2 (1993): 338-343.